

Supporting Information: Predictive Machine Learning Models Trained on Experimental Datasets for Electrochemical Nitrogen Reduction

Darik A. Rosser^{1,2}, Brianna R. Farris^{1,2}, and Kevin C. Leonard^{1,2,*}

¹Department of Chemical & Petroleum Engineering 4132 Learned Hall 1530 W 15th St, ,
The University of Kansas, Lawrence, KS USA

²Center for Environmentally Beneficial Catalysis 1501 Wakarusa Dr. LSRL Building A,
Suite 110, , The University of Kansas, Lawrence, KS USA

*kcleonard@ku.edu

Number of Pages: 10 Number of Figures: 12 Number of Tables: 1

Contents

1 Machine Learning Results	S2
1.1 Partial Decision Trees	S2
1.2 Feature Classifications	S3
1.3 Max Depth Determination	S4
1.4 Random Seed Testing	S6
1.5 Label Encoded Results	S8
1.6 Machine Learning Methods	S9

List of Figures

S1a Efficiency regression decision tree shown with a depth of 3	S2
S1b Rate regression decision tree shown with a depth of 3	S2
S2a Max depth vs the Accuracy for the decision tree Efficiency Regression	S4
S2b Max depth vs the Accuracy for the decision tree Rate Regression	S4
S2c Max depth vs the Accuracy for the random forest Efficiency Regression	S5
S2d Max depth vs the Accuracy for the random forest Rate Regression	S5
S3a Variance in cross validated standard deviation detected using 10 random seeds.	S6
S3b Averaged single pass accuracy showing testing vs training using 10 random seeds.	S6
S3c Averaged cross validated accuracy using 10 random seeds.	S7
S4a Diagonal plots showing results for label encoded Decision Trees, Random Forests and Linear Regressions	S8
S4b Scoring for label encoded Decision Trees, Random Forests and Linear Regressions	S8

List of Tables

S1 Unique Categorical Features	S3
--	----

1 Machine Learning Results

1.1 Partial Decision Trees

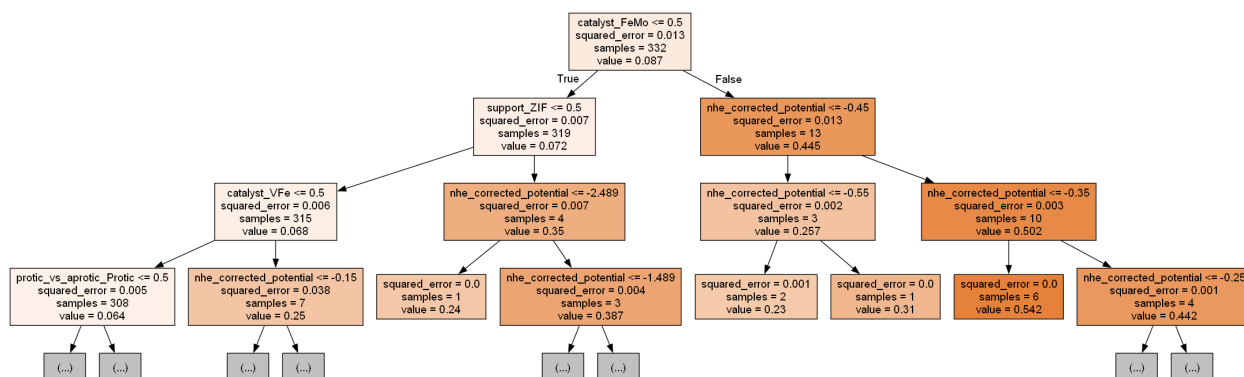


Figure S1a. Efficiency regression decision tree shown with a depth of 3

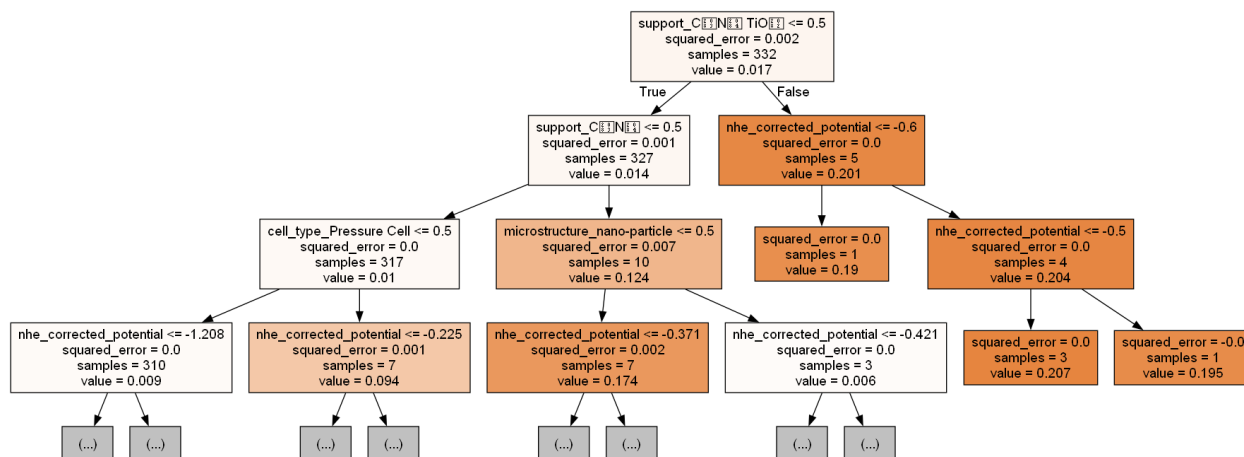


Figure S1b. Rate regression decision tree shown with a depth of 3

1.2 Feature Classifications

Table S1. Unique Categorical Features

Category	Features
Catalyst	C ₃ N ₄ , Au, Nb ₂ O ₅ , Ru, Ag/Pd, Pt, Fe ₂ O ₃ , MoS ₂ , Co, VN/CC, B ₄ C, WS ₂ WO ₂ , Rh, CoP-MoP, Fe ₃ O ₄ , K ₃ Ti ₈ O ₁₇ , VFe, Bi, Mo ₂ C, FeMo, Fe ₃ O ₄ /Bi, Fe, Pd, Zn, VS ₂ , MOSe ₂ , Cu, Mn, CrN, C, Ir
Atomic Number	6, 79, 41, 44, 47, 78, 26, 42, 27, 23, 5, 22, 83, 45, 46, 30, 29, 25, 74, 24, 77
Electrode	Carbon Paper, carbon membrane, TiO ₂ , BCY, Carbon Cloth, Glassy Carbon, Catalyst, Au
Support	unsupported, carbon nanotube, Carbon, C ₃ N ₄ , TiO ₂ , rGO, NC, FeS ₂ /C, BiClO, MnO ₂ , Graphdiyne, Carbon Fiber, TCPP, MoSe ₂ , TPP, C ₃ N ₄ /TiO ₂ , Mxene, RGO, ZIF
Dopant	Yes, No
Micro-Structure	Nanorod, Agglomerated, Nanoparticle, Nanosheet, Nanocage, Nanofiber, Heterostructured, Single Atom, Nanosphere, Amorphous, Microsphere, Polycrystalline
Cell Type	Traditional, Solid State, Pressure Cell
Electrolyte	NaClO ₄ , LiClO ₄ , HCl, Na ₂ SO ₄ , H ₂ SO ₄ , KOH, BCY, KClO ₄ , CsH ₂ PO ₄ , K ₂ SO ₄ , lithium trifluoromethanesulfonate
Protic vs Aprotic	Protic, Aprotic

1.3 Max Depth Determination

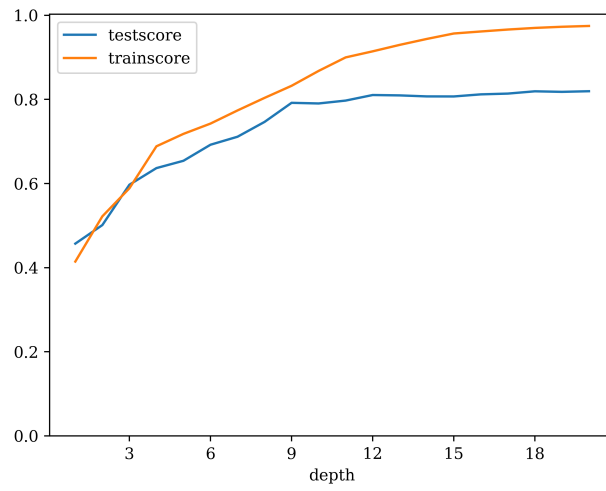


Figure S2a. Max depth vs the Accuracy for the decision tree Efficiency Regression

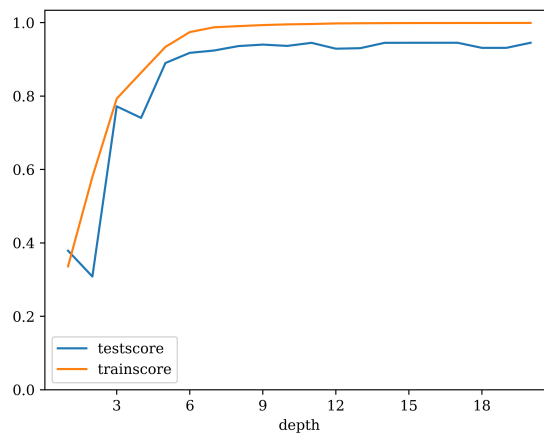


Figure S2b. Max depth vs the Accuracy for the decision tree Rate Regression

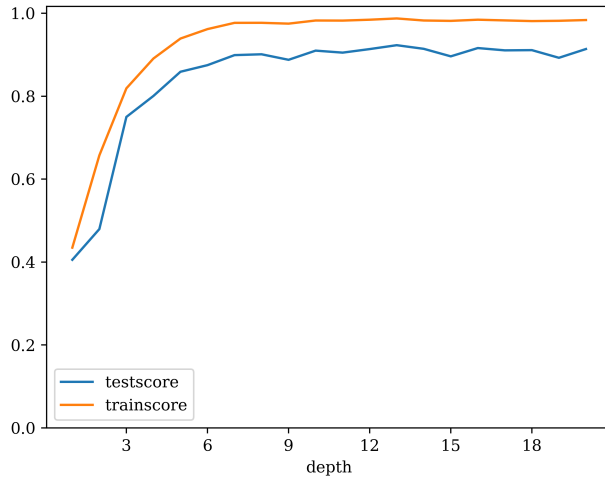


Figure S2c. Max depth vs the Accuracy for the random forest Efficiency Regression

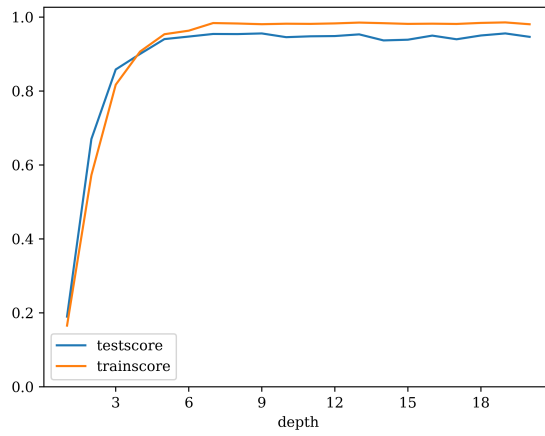


Figure S2d. Max depth vs the Accuracy for the random forest Rate Regression

1.4 Random Seed Testing

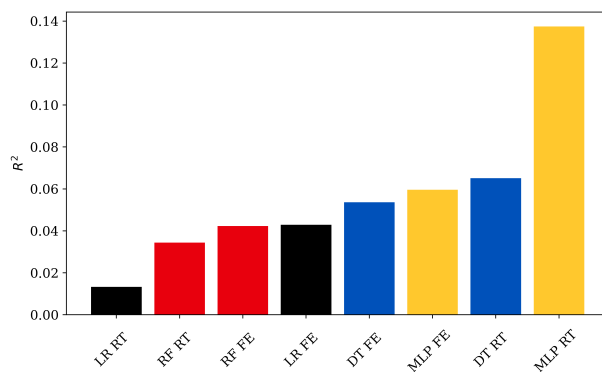


Figure S3a. Variance in cross validated standard deviation detected using 10 random seeds.

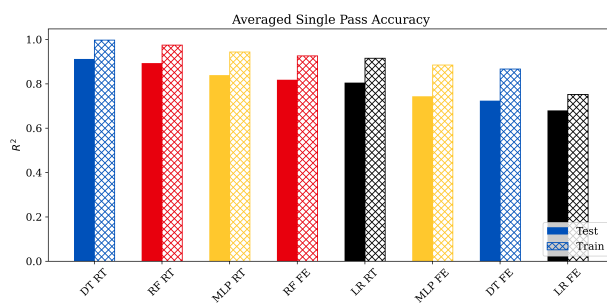


Figure S3b. Averaged single pass accuracy showing testing vs training using 10 random seeds.

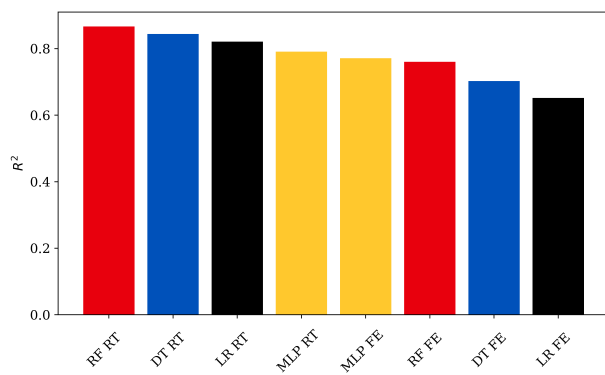


Figure S3c. Averaged cross validated accuracy using 10 random seeds.

1.5 Label Encoded Results

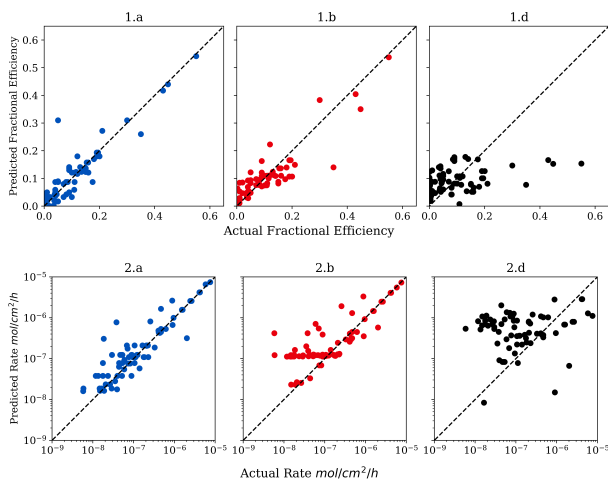


Figure S4a. Diagonal plots showing results for label encoded Decision Trees, Random Forests and Linear Regressions

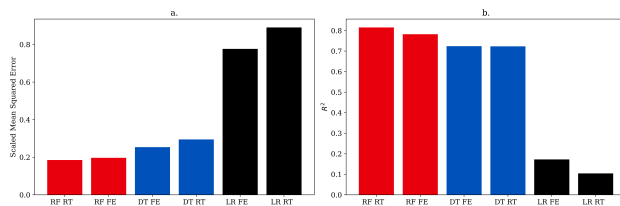


Figure S4b. Scoring for label encoded Decision Trees, Random Forests and Linear Regressions

1.6 Machine Learning Methods

This section will review the procedure for using the attached machine learning models for analyzing electrochemical Nitrogen Reduction Reactions. All software, functions and programming used for this analysis are attached and open for public use and study. Run the IPYNB files in this order: DataProcessing, All Models Exporting Data and Discussion. The first file, Data Processing, is used to condition the data-set for machine learning. The second file does the bulk of the machine learning work. When running the second file we strongly recommend attempting to use our data-set first. If the data-set is altered then the Keras Tuners attached to the MLP neural networks will need to be re-run by setting their "Overwrite" parameter to "True". Tuning neural networks is a time intensive process which can be expedited by applying GPU instead of CPU - however GPU may have lower physical memory than CPU which leads to smaller neural nets. Thus the tuning parameters may need to be altered depending on hardware and time constraints. Finally, the Discussion file will provide useful graphics to understand the outputs of each machine learning model.

Database References

- (1) Song, Y. et al. A physical catalyst for the electrolysis of nitrogen to ammonia. *Science Advances* **2018**, *4*, DOI: 10.1126/SCIADV.1700336/SUPPL_FILE/1700336_SM.PDF.
- (2) Wang, H.; Wang, L.; Wang, Q.; Ye, S.; Sun, W.; Jiang, Z.; Qiao, Q.; Zhu, Y.; Song, P.; Li, D.; He, L.; Zhang, X.; Yuan, J.; Ozin, G. A. Ambient Electrosynthesis of Ammonia: Electrode Porosity and Composition Engineering. *Angewandte Chemie International* **2018**, *57*, DOI: 10.1002/ange.201805514.
- (3) Han, J.; Liu, Z.; Ma, Y.; Cui, G.; Xie, F.; Wang, F.; Wu, Y.; Gao, S.; Xu, Y.; Sun, X. Ambient N₂ fixation to NH₃ at ambient conditions: Using Nb₂O₅ nanofiber as a high-performance electrocatalyst. *Nano Energy* **2018**, *52*, 264–270.
- (4) Kishira, S.; Qing, G.; Suzu, S.; Kikuchi, R.; Takagaki, A.; Oyama, S. T. Ammonia synthesis at intermediate temperatures in solid-state electrochemical cells using cesium hydrogen phosphate based electrolytes and noble metal catalysts. *International Journal of Hydrogen Energy* **2017**, *42*, 26843–26854.
- (5) Qing, G.; Kikuchi, R.; Kishira, S.; Takagaki, A.; Sugawara, T.; Oyama, S. T. Ammonia Synthesis by N₂ and Steam Electrolysis in Solid-State Cells at 220°C and Atmospheric Pressure. *Journal of The Electrochemical Society* **2016**, *163*, E282–E287.
- (6) Xiang, X.; Wang, Z.; Shi, X.; Fan, M.; Sun, X. Ammonia Synthesis from Electrocatalytic N₂ Reduction under Ambient Conditions by Fe₂O₃ Nanorods. *ChemCatChem* **2018**, *10*, 4530–4535.
- (7) Wang, X. et al. Atomically dispersed Au₁ catalyst towards efficient electrochemical synthesis of ammonia. *Science Bulletin* **2018**, *63*, 1246–1253.
- (8) Shi, M. M.; Bao, D.; Wulan, B. R.; Li, Y. H.; Zhang, Y. F.; Yan, J. M.; Jiang, Q. Au Sub-Nanoclusters on TiO₂ toward Highly Efficient and Selective Electrocatalyst for N₂ Conversion to NH₃ at Ambient Conditions. *Advanced Materials* **2017**, *29*, 1606550.
- (9) Chen, S.; Perathoner, S.; Ampelli, C.; Mebrahtu, C.; Su, D.; Centi, G. Electrocatalytic Synthesis of Ammonia at Room Temperature and Atmospheric Pressure from Water and Nitrogen on a Carbon-Nanotube-Based Electrocatalyst. *Angewandte Chemie* **2017**, *129*, 2699–2703.
- (10) Kosaka, F.; Nakamura, T.; Otomo, J. Electrochemical Ammonia Synthesis Using Mixed Protonic-Electronic Conducting Cathodes with Exsolved Ru-Nanoparticles in Proton Conducting Electrolysis Cells. *Journal of The Electrochemical Society* **2017**, *164*, F1323–F1330.
- (11) Zhang, L. et al. Electrochemical Ammonia Synthesis via Nitrogen Reduction Reaction on a MoS₂ Catalyst: Theoretical and Experimental Studies. *Advanced Materials* **2018**, *30*, 1800191.
- (12) Imamura, K.; Kubota, J. Electrochemical membrane cell for NH₃ synthesis from N₂ and H₂O by electrolysis at 200 to 250 °C using a Ru catalyst, hydrogen-permeable Pd membrane and phosphate-based electrolyte. **2018**, DOI: 10.1039/c8se00054a.
- (13) Bao, D. et al. Electrochemical Reduction of N₂ under Ambient Conditions for Artificial N₂ Fixation and Renewable Energy Storage Using N₂/NH₃ Cycle. *Advanced Materials* **2017**, *29*, 1604799.
- (14) Kim, K.; Yoo, C.-Y.; Kim, J.-N.; Yoon, H. C.; Han, J.-I. Electrochemical Synthesis of Ammonia from Water and Nitrogen in Ethylenediamine under Ambient Temperature and Pressure. *Journal of The Electrochemical Society* **2016**, *163*, F1523–F1526.

- (15) Bicer, Y.; Dincer, I. Electrochemical Synthesis of Ammonia in Molten Salt Electrolyte Using Hydrogen and Nitrogen at Ambient Pressure. *Journal of The Electrochemical Society* **2017**, *164*, H5036–H5042.
- (16) Guo, W.; Liang, Z.; Zhao, J.; Zhu, B.; Cai, K.; Zou, R.; Xu, Q. Hierarchical Cobalt Phosphide Hollow Nanocages toward Electrocatalytic Ammonia Synthesis under Ambient Pressure and Room Temperature. *Small Methods* **2018**, *2*, 1800204.
- (17) Qiu, W.; Xie, X. Y.; Qiu, J.; Fang, W. H.; Liang, R.; Ren, X.; Ji, X.; Cui, G.; Asiri, A. M.; Cui, G.; Tang, B.; Sun, X. High-performance artificial nitrogen fixation at ambient conditions using a metal-free electrocatalyst. *Nature Communications 2018 9:1* **2018**, *9*, 1–8.
- (18) Zhang, X.; Kong, R. M.; Du, H.; Xia, L.; Qu, F. Highly efficient electrochemical ammonia synthesis via nitrogen reduction reactions on a VN nanowire array under ambient conditions. *Chemical Communications* **2018**, *54*, 5323–5325.
- (19) Liang, W.; Qin, W.; Li, D.; Wang, Y.; Guo, W.; Bi, Y.; Sun, Y.; Jiang, L. Localized surface plasmon resonance enhanced electrochemical nitrogen reduction reaction. *Applied Catalysis. B, Environmental* **2022**, *301*, 120808.
- (20) Liu, Y.; Tao, Y.; Lu, Z.; Teng, J.; Hao, W.; Lin, J.; Li, G. NaCl template-assisted construction of a CoP-MoP heterostructured electrocatalyst for electrocatalytic nitrogen reduction. *Dalton Transactions* **2023**, *52*, 11631–11637.
- (21) Wang, F.; Xia, L.; Li, X.; Yang, W.; Zhao, Y.; Mao, J. Nano-Ferric Oxide Embedded in Graphene Oxide: High-performance Electrocatalyst for Nitrogen Reduction at Ambient Condition. *Energy & Environmental Materials* **2021**, *4*, 88–94.
- (22) Sebastian, M.; Das, S.; Gopalan, N. K. Nitrogen reduction reaction under ambient conditions by K₃Ti₈O₁₇ nanorod electrocatalyst. *Sustainable Energy & Fuels* **2022**, *6*, 1519–1528.
- (23) Wang, Y.; Wang, J.; Li, H.; Li, Y.; Li, J.; Wei, K.; Peng, F.; Gao, F. Nitrogen Reduction Reaction: Heteronuclear Double-Atom Electrocatalysts. *Small structures* **2023**, *4*, n/a.
- (24) Wan, Y.; Zhou, H.; Zheng, M.; Huang, Z.-H.; Kang, F.; Li, J.; Lv, R. Oxidation State Modulation of Bismuth for Efficient Electrocatalytic Nitrogen Reduction to Ammonia. *Advanced Functional Materials* **2021**, *31*, 2100300.
- (25) Fan, B.; Wang, H.; Zhang, H.; Song, Y.; Zheng, X.; Li, C.; Tan, Y.; Han, X.; Deng, Y.; Hu, W. Phase Transfer of Mo₂C Induced by Boron Doping to Boost Nitrogen Reduction Reaction Catalytic Activity. *Advanced functional materials* **2022**, *32*, n/a.
- (26) Wang, X.; Feng, Z.; Xiao, B.; Zhao, J.; Ma, H.; Tian, Y.; Pang, H.; Tan, L. Polyoxometalate-based metal-organic framework-derived bimetallic hybrid materials for upgraded electrochemical reduction of nitrogen. *Green Chemistry* **2020**, *22*, 6157–6169.
- (27) Li, X.; Xue, C.; Zhou, X.; Wei, Y.; Yu, Y.; Fu, Y.; Liu, W.; Lan, Y. Polyoxometalate-derived bimetallic catalysts for the nitrogen reduction reaction. *Materials Chemistry Frontiers* **2023**, *7*, 72–727.
- (28) Huang, T.; Liu, Z.; Zhang, Y.; Wang, F.; Wen, J.; Wang, C.; Hossain, M.; Xie, Q.; Yao, S.; Wu, Y. Promoting electrocatalytic nitrogen reduction to ammonia via Fe-boosted nitrogen activation on MnO₂ surfaces. *Journal of Materials Chemistry* **2020**, *8*, 13679–13684.
- (29) Suryanto, B. H.; Kang, C. S.; Wang, D.; Xiao, C.; Zhou, F.; Azofra, L. M.; Cavallo, L.; Zhang, X.; Macfarlane, D. R. Rational Electrode-Electrolyte Design for Efficient Ammonia Electrosynthesis under Ambient Conditions. *ACS Energy Letters* **2018**, *3*, 1219–1224.

- (30) Zou, H.; Rong, W.; Wei, S.; Ji, Y.; Duan, L. Regulating kinetics and thermodynamics of electrochemical nitrogen reduction with metal single-atom catalysts in a pressurized electrolyser. *Proceedings of the National Academy of Sciences* **2020**, *117*, 29462–29468.
- (31) Wang, Y.; Ma, Z.; Liu, K.; Yang, X.; Wang, J.; Wang, X. Rigid anchoring of highly crystallized and uniformly dispersed Pd nanocrystals on carbon fibers for ambient electrocatalytic reduction of nitrogen to ammonia. *Dalton Transactions* **2021**, *5*, 6975–6981.
- (32) Cong, M.; Chen, X.; Xia, K.; Ding, X.; Zhang, L.; Jin, Y.; Gao, Y.; Zhang, L. Selective nitrogen reduction to ammonia on iron porphyrin-based single-site metal-organic frameworks. *Journal of Materials Chemistry* **2021**, *9*, 4673–4678.
- (33) Xu, X.; Wang, Y.; Chen, X.; Qian, X.; Liang, Z.; Cui, H.; Tian, J.; Shao, M. Semi-metal 1T phase MoS₂ nanosheets for promoted electrocatalytic nitrogen reduction. *EcoMat* **2021**, *3*, e12122.
- (34) Zhao, L.; Xiong, Y.; Wang, X.; Zhao, R.; Chi, X.; Zhou, Y.; Wang, H.; Yang, Z.; Yan, Y.-M. Shearing Sulfur Edges of VS₂ Electrocatalyst Enhances its Nitrogen Reduction Performance. *Small* **2022**, *18*, e2106939.
- (35) Sun, S.; Yang, X.; Li, S.; Chen, X.; Li, K.; Lv, J.; Wang, W.; Cheng, D.; Yong-Hui, W.; Hong-Ying, Z. Single-atom metal–N₄ site molecular electrocatalysts for ambient nitrogen reduction. *Catalysis Science & Technology* **2021**, *11*, 2589–2596.
- (36) Chen, D.; Luo, M.; Ning, S.; Lan, J.; Peng, W.; Lu, Y.-R.; Chan, T.-S.; Tan, Y. Single-Atom Gold Isolated Onto Nanoporous MoSe₂ for Boosting Electrochemical Nitrogen Reduction. *Small* **2022**, *18*, e2104043.
- (37) Wu, X.; Tang, L.; Si, Y.; Ma, C.; Zhang, P.; Yu, J.; Liu, Y.; Ding, B. Smart Interfacing between Co-Fe Layered Double Hydroxide and Graphitic Carbon Nitride for High-efficiency Electrocatalytic Nitrogen Reduction. *Energy & Environmental Materials* **2023**, *6*, n/a.
- (38) Ling, Y.; Kazim, F. M.; Ma, S.; Zhang, Q.; Qu, K.; Wang, Y.; Xiao, S.; Cai, W.; Yang, Z. Strain induced rich planar defects in heterogeneous WS₂/WO₂ enable efficient nitrogen fixation at low overpotential. *Journal of Materials Chemistry A* **2020**, *8*, 12996–13003.
- (39) Ma, Z.; Chen, J.; Luo, D.; Thersleff, T.; Dronskowski, R.; Slabon, A. Structural evolution of CrN nanocube electrocatalysts during nitrogen reduction reaction. *Nanoscale* **2020**, *12*, 19276–19283.
- (40) Liu, H. M.; Han, S. H.; Zhao, Y.; Zhu, Y. Y.; Tian, X. L.; Zeng, J. H.; Jiang, J. X.; Xia, B. Y.; Chen, Y. Surfactant-free atomically ultrathin rhodium nanosheet nanoassemblies for efficient nitrogen electroreduction. *Journal of Materials Chemistry A* **2018**, *6*, 3211–3217.
- (41) Yang, Y.; Zhang, L.; Hu, Z.; Zheng, Y.; Tang, C.; Chen, P.; Wang, R.; Qiu, K.; Mao, J.; Ling, T.; Qiao, S.-Z. The Crucial Role of Charge Accumulation and Spin Polarization in Activating Carbon-Based Catalysts for Electrocatalytic Nitrogen Reduction. *Angewandte Chemie (International ed.)* **2020**, *59*, 4525–4531.
- (42) Liu, A.; Liang, X.; Zhu, H.; Ren, X.; Gao, L.; Gao, M.; Yang, Y.; Li, G.; Ma, T. Two-Dimensional MXene Supported Bismuth for Efficient Electrocatalytic Nitrogen Reduction. *ChemCatChem* **2022**, *14*, e202101683.
- (43) Wang, W.; Wang, X.; Sun, Y.; Tian, Y.; Liu, X.; Chu, K.; Li, J. Ultrasmall iridium nanoparticles on graphene for efficient nitrogen reduction reaction. *New journal of chemistry* **2022**, *46*, 5464–5469.

- (44) Sim, H. Y. F.; Chen, J. R. T.; Koh, C. S. L.; Lee, H. K.; Han, X.; Phan-Quang, G. C.; Pang, J. Y.; Lay, C. L.; Pedireddy, S.; Phang, I. Y.; Yeow, E. K. L.; Ling, X. Y. ZIF-Induced d-Band Modification in a Bimetallic Nanocatalyst: Achieving Over 44% Efficiency in the Ambient Nitrogen Reduction Reaction. *Angewandte Chemie (International ed.)* **2020**, *59*, 16997–17003.